

Effects of Magnetic Fields on Radiatively Overstable Shock Waves

Paul A. Kimoto

Department of Physics, Cornell University, Ithaca, NY 14853

and

David F. Chernoff

Department of Astronomy, Cornell University, Ithaca, NY 14853

accepted by The Astrophysical Journal
©1997 The American Astronomical Society

ABSTRACT

We discuss high-resolution simulations of one-dimensional, plane-parallel shock waves with mean speeds between 150 and 240 km s⁻¹ propagating into gas with Alfvén velocities up to 40 km s⁻¹ and outline the conditions under which these radiative shocks experience an oscillatory instability in the cooling length, shock velocity, and position of the shock front. We investigate two forms of postshock cooling: a truncated single power law and a more realistic piecewise power law. The degree of nonlinearity of the instability depends strongly on the cooling power law and the Alfvén Mach number: for power-law indices $\alpha < 0$ typical magnetic field strengths may be insufficient either to stabilize the fundamental oscillatory mode or to prevent the oscillations from reaching nonlinear amplitudes.

Subject headings: hydrodynamics—instabilities—shock waves

1. Introduction

Work by Langer, Chanmugam, & Shaviv (1981), Chevalier & Imamura (1982), and Imamura, Wolff, & Durisen (1984) shows that the physical structure of some radiative shocks and their cooling regions is subject to a cooling overstability. The shock velocity and the length of the cooling column of postshock gas may oscillate instead of evolving in a steady manner. The linear perturbative analysis of Chevalier & Imamura, which assumes power-law cooling laws $\Lambda \propto \rho^2 T^\alpha$, indicates that one-dimensional nonmagnetic shocks are *stable* when α is sufficiently large, $\alpha \gtrsim 0.8$. If the cooling rises rapidly with temperature, perturbations to a cooling region in steady state that increase the shock velocity v_s cause more rapid cooling and require shorter cooling lengths, and the shock is stable against perturbations. On the other hand, if the cooling law does not rise

sufficiently rapidly with temperature, then the cooling length oscillates overstably between fast shocks with long cooling lengths and slow shocks with short cooling lengths.

Tóth & Draine (1993) extend the perturbative analysis to include a frozen one-dimensional magnetic field, oriented perpendicular to the gas motion and uniform in the upstream gas. Compression at the shock front tends to align the postshock magnetic field with the plane of the shock. The field’s contribution to the total pressure tends to stabilize oscillations.

In this paper we discuss sets of one-dimensional, plane-parallel simulations of radiative shocks, both with and without the transverse magnetic field. Shocks in the interstellar medium propagating faster than approximately 150 km s^{-1} are candidates for these instabilities. For example, the blast waves of supernova remnants may pass through a velocity range in which the shock velocities are high enough and the cooling times short enough, compared with the remnant age, for these oscillations to occur (Kimoto & Chernoff 1997). For cooling laws we adopt $\Lambda = n_{\text{H}}^2 f(T)$, where n_{H} is the hydrogen-nuclei density. For the cooling function $f(T)$ we use either (1) single power laws or (2) a piecewise power-law fit (for temperatures above $3 \times 10^4 \text{ K}$) to the result of Raymond, Cox, & Smith (1976).

We note that the latter cooling function assumes that the emitting plasma is in collisional equilibrium. However, because collisional, ionization, and recombination rates are slow compared to the cooling rate, an accurate evaluation of the cooling necessitates a time-dependent treatment of the ionization evolution. Several specific cases of one-dimensional simulations incorporating explicit evolution of ionization states are discussed by Innes, Giddings, & Falle (1987), Gaetz, Edgar, & Chevalier (1988), and Innes (1992). Of these three papers, only Innes (1992) incorporates a transverse magnetic field. Such treatments are computationally very demanding. By using simpler cooling laws, we are able to investigate a wider range of parameter space in mean shock speed and magnetic field strength, as well as assess the sensitivity of the results to the form of the cooling law. Our qualitative conclusions should apply to more accurate treatments as well.

Our piecewise power-law cooling function differs from that of Tóth & Draine (1993) as discussed below, and our results differ qualitatively from their similar suite of calculations. Because our cooling function is more unstable for mean shock velocities between 150 km s^{-1} and 210 km s^{-1} , we find that the stabilizing effect of magnetic fields is reduced. In our analysis, larger magnetic fields are necessary to stabilize large-amplitude, fundamental-mode oscillations, and as well to stabilize all oscillatory modes. We do not claim that our treatment leads to results that are physically more reliable: the differences between the two sets of results serve to point out that quantitative results will require a more precise treatment of the cooling.

Most recently, Walder & Folini (1996) discuss spherically symmetric, one-dimensional, high-resolution simulations of the radiative cooling instability. Like ours, these simulations use a piecewise power-law cooling function. They identify five qualitatively distinct oscillation types. We note that the two types that we discuss in some detail below correspond to the “strong forms” that they describe for the fundamental and first overtone modes. We do not draw further parallels

with their work, however, since their simulations do not include magnetic fields, an essential ingredient in our discussion.

In the following section we discuss simulations carried out with our two cooling functions in parameter spaces in which we vary the magnetic field strength and properties of the cooling function. We identify two distinct types of nonlinear oscillations: one in which the fundamental mode dominates the motion, and one in which the first-overtone mode dominates. In the final section we summarize and draw conclusions based on our results, taking into account the limitations of the systems we have studied.

2. Simulations of oscillations

2.1. Equations of motion and initial conditions

In order to study the oscillatory cycles of this cooling overstability, we consider one-dimensional, plane-parallel systems of ideal (inviscid and with zero thermal conductivity), infinitely conducting gases, with a magnetic field perpendicular to the direction of motion. Our cooling law takes the form $\Lambda = n_{\text{H}}^2 f(T)$. To simplify the investigation of the oscillatory behavior, in some cases we adopt for $f(T)$ single power laws (with low-temperature cutoffs). In the other cases, as an approximation to a realistic cooling function, we use for $f(T)$ a piecewise power-law fit to the result of Raymond et al. (1976). To account for the turnoff of cooling when the gas reaches a sufficiently low temperature to recombine, we arrange for the cooling to vanish below a cutoff temperature $T_c \approx 2 \times 10^4$ K. Figure 1 shows the function we adopt, as well as the function used for application to the interstellar medium by Tóth & Draine (1993). The points indicated in the figure denote the shock temperatures of steady-state shocks (in the absence of magnetic fields) with velocities 150, 180, 210, and 240 km s⁻¹.

Since the cooling law takes this simple functional form, the length and time scales of solutions are simply proportional to $1/n_{\text{H}}^{\text{in}}$, and all densities, pressures, and energies proportional to n_{H}^{in} . Because of this scaling, the particular value we choose for the upstream density is arbitrary, and so usually we quote values in terms of n_{H}^{in} (omitting the superscript “in” where there is no ambiguity).

Our numerical calculations use an Eulerian finite-difference algorithm that can evolve flows with strong shocks and gradients. We use operator splitting to separate the cooling from the magnetohydrodynamics, in which we evolve four conserved densities (ρ , ρv , e_{tot} , and B) with a flux-corrected transport scheme (Zalesak 1979). A multigrid method using some ideas of Berger & Colella (1989) allows us to place high resolution on localized parts of the flow as required for numerical accuracy. Details of the methods may be found in the Appendix of Kimoto & Chernoff (1997).

In all of the simulations, supersonic gas of temperature 2500 K flows uniformly into one end

of the computational domain and is shocked. This gas is assumed to be completely preionized by the photons emitted near the shock and to contain helium in a 1:10 ratio to hydrogen. (In our simulations, we give the inflowing gas a hydrogen-nuclei density of $n_{\text{H}}^{\text{in}} = 50 \text{ cm}^{-3}$, but because of the scaling properties of our equations of motion, the particular value has no significance.) Although the temperature of our unshocked gas is unrealistic both for preionized gas and for a quiescent interstellar medium, the dynamics of the shock and the cooling column is unaffected as long as the shock is strong. The gas cools and accumulates near a wall at the other end, where we impose a perfectly reflecting boundary condition. When the cooling region evolves in a steady state, the quiescent, fully cooled gas builds up at the wall, and the cooling region moves outward at constant velocity. We find considerably more complicated dynamics.

The initial conditions are constructed to correspond closely with the steady-state cooling flow for a given shock speed and upstream Alfvén velocity. The main ingredient is a numerical solution to the equations of motion, generated by working in the shock frame and assuming no time dependence. First, this steady-state solution is truncated at a point where the gas has approximately attained its final cooled, dense state (beyond the main part of the cooling column), and second, the transition between upstream and shocked gas is smoothed slightly. The numerical evolution scheme smooths discontinuities over several gridpoints. By necessity the smoothing that we employ in generating initial conditions differs slightly from the smoothing developed under the numerical scheme. We then transform the solution into the frame of the cold, dense gas that builds up at the wall boundary. In most cases the inflow velocity is only slightly less than the average shock speed since the gas compresses strongly. During the highly nonlinear oscillations the conditions of the cooling column do not resemble those of the steady state, and waves are driven downstream into the cooled, dense gas. We find, however, that the measured average shock propagation speed fluctuates only slightly about the shock speed of the steady-state initial condition. Table 1 lists the results for twenty cases discussed below—covering mean shock speeds from 150 to 240 km s^{-1} and upstream Alfvén velocities up to 20 km s^{-1} —that use the piecewise power-law cooling function.

2.2. Parameter space and instability types

The linear perturbative analysis of Chevalier & Imamura (1982), which assumes $f(T) \propto T^\alpha$ and no magnetic field, yields a discrete spectrum of modes for motions of the cooling column. The fundamental mode has frequency

$$\nu_F \approx \frac{v_s}{21 L_{\text{cool}}}, \quad (1)$$

and the overtone frequencies are approximately odd multiples of the fundamental. The overtone modes are unstable over a greater range of cooling power laws than is the fundamental.

A transverse magnetic field can stabilize the oscillations. The perturbative analysis of Tóth &

Draine (1993), which incorporates such a magnetic field, uses a cooling function

$$f_{\text{TD}}(T) \propto \begin{cases} T^\alpha & \text{if } T > T_t, \\ T^{1/2} & \text{if } T < T_t, \end{cases} \quad (2)$$

for some turnover temperature T_t . For shock temperatures much greater than T_t , the minimum stabilizing magnetic field depends mainly on α : the field is greater for smaller values of α (i.e., the more unstable cases), and it is greater for overtone modes than for the fundamental. In addition, the stabilizing field for all overtone modes is approximately the same. In nonlinear calculations typically only the first overtone mode is observed. The results can be summarized as follows: the minimum stabilizing field for mode i may be parameterized by $M_{A,i}^{-1}$ (where the Alfvén Mach number is $M_A = v_s/v_A$, the Alfvén velocity is $v_A = B/(4\pi\rho_{\text{in}})^{1/2}$, and the upstream density is ρ_{in}). For small magnetic fields, $M_A^{-1} < M_{A,F}^{-1} < M_{A,O}^{-1}$, both fundamental and overtone modes are unstable; for intermediate fields, $M_{A,F}^{-1} < M_A^{-1} < M_{A,O}^{-1}$, only the overtones are unstable; and for large fields, $M_{A,F}^{-1} < M_{A,O}^{-1} < M_A^{-1}$, all modes are stable. The short dotted lines in Figure 2 show approximately the $M_{A,F}^{-1}$ (lower) and $M_{A,O}^{-1}$ (upper) curves in the (α, M_A^{-1}) parameter space as calculated by Tóth & Draine using the cooling function (eq. [2]) with turnover temperature $T_t = 10^{-3}\mu v_s^2/k_B$, where μ is the mean particle mass and v_s is the mean shock speed.

2.3. Oscillations without magnetic fields

As background, we begin by describing properties of oscillations in the absence of magnetic fields. For simulations adopting the piecewise power-law cooling function, Table 2 lists typical amplitudes (minimum to maximum shock velocities) and periods for a range of shock speeds—from 130 to 240 km s^{-1} —that should cover a range of supernova remnants with oscillating shocks (Kimoto & Chernoff 1997). The corresponding range of shock temperatures covers a break in the power-law fit (locally proportional to T^α) that enters our cooling function: Above 5×10^5 K, which corresponds to a 190 km s^{-1} shock (neglecting magnetic fields), $\alpha \approx -0.1$; from 2.5×10^5 to 5×10^5 K, we adopt $\alpha \approx -2.2$ (for which the oscillations are more unstable).

From these simulations we make several observations that are generally consistent with the results of previous work done with a variety of steep cooling laws (e.g., Imamura, Wolff, & Durisen 1984; Innes, Giddings, & Falle 1987; Gaetz, Edgar & Chevalier 1988; Walder & Folini 1996). The instability is so strong that within a few periods the oscillations develop and their amplitudes quickly saturate. When the oscillations become nonlinear, the fundamental mode dominates. Our amplitudes and periods typically vary by up to 10%, but the values indicated in Table 2 should be representative. The period of the fundamental mode is close to $\tau_F = 21 L_{\text{cool}}/\langle v_s \rangle$, approximately the value (cf. eq. [1]) predicted by linear analysis (Chevalier & Imamura 1982). We show this approximate value for comparison in Table 2, where (in the spirit of small-amplitude analysis) we take L_{cool} from the steady-state solutions. (In the perturbative treatments the gas cools to $T = 0$ [for analytic convenience]; our cooling function turns off in a tapered manner at a finite temperature [in part, for numerical convenience]. Because the gas

cools rapidly as it reaches high densities, it is still possible to identify a “cooling length” without much ambiguity.) In our simulations the oscillations become highly nonlinear, and the oscillatory periods are somewhat longer than the linear-analysis values.

2.4. Oscillations affected by magnetic fields

Next we consider simulations with a transverse magnetic field. For simplicity we begin by considering cooling functions with single power laws in order to investigate the effects of power-law slope and magnetic field on the selection of the dominant mode. For a cooling function (cf. eq. [2]) we use

$$f_{\text{PL}}(T) \propto \begin{cases} T^\alpha & \text{if } T > T_t, \\ T^{1/2} \left\{ \frac{1}{2} + \frac{1}{2} \tanh\left[\frac{(T - \frac{9}{14}T_t)}{(\frac{1}{49}T_t)}\right] \right\} & \text{if } T < T_t. \end{cases} \quad (3)$$

The quantity in braces arranges for the cooling to effectively vanish at small temperatures ($T < 9T_t/14$). For $\alpha \geq -0.5$ we (like Tóth & Draine [1993]) set the turnover temperature so that $k_B T_t / (\mu v_s^2) = 10^{-3}$. For $\alpha \leq -0.8$, however, we use $k_B T_t / (\mu v_s^2) = 10^{-2}$ for numerical convenience.

In the previous subsection we noted that the fundamental mode dominates the oscillations in the absence of magnetic fields ($M_A^{-1} = 0$). At several values of the power-law index α (namely, -1 , -0.8 , -0.5 , -0.3 , 0 , and 0.3), we bracket the reciprocal Alfvén Mach number \mathcal{M}_A^{-1} at which dominance switches from the fundamental to an overtone mode. Simulations yield the limits in \mathcal{M}_A^{-1} shown as line segments in Figure 2, and the curve in long-dashed lines (drawn only for illustrative purposes) shows approximately the behavior of \mathcal{M}_A^{-1} . Naturally this curve must lie below the lower short-dashed line, which denotes $M_{A,F}^{-1}$, the value at which the fundamental mode is marginally stable in the linear analysis of Tóth & Draine. We note that the magnitude of \mathcal{M}_A^{-1} curve is clearly distinct from that of $M_{A,F}^{-1}$.

Tóth & Draine discuss the results of hydrodynamical simulations with the values of $\alpha \geq 0$ and $M_A^{-1} \geq 0.03$ denoted by dots in Figure 2. They observe that the first-overtone mode dominates whenever the flow is unstable and that the oscillations have amplitudes $\lesssim 10\%$. We have performed several simulations in the vicinity of the dots using our version of the power-law cooling function (eq. [3]), and these confirm their conclusions. However, Figure 2 also shows that *the fundamental mode dominates the oscillations over an astrophysically significant range of magnetic fields when $\alpha < 0$* . Even the simplest forms of cooling functions (e.g., as shown in Fig. 1) require temperature ranges in which locally $\alpha < 0$. In addition, for $\alpha < 0$ the oscillations are decidedly nonlinear: when the fundamental mode dominates, the velocity fluctuations (minimum to maximum) are at least 50% of the mean shock velocity. In the handful of cases we have simulated in which the overtone mode dominates (i.e., with M_A^{-1} slightly greater than \mathcal{M}_A^{-1}), the velocity fluctuations are typically $\sim 25\%$. Figure 3 shows the magnitude of fluctuations in cooling-column length and shock velocity (relative to the steady-state values) as a function of M_A^{-1} when $\alpha = -0.8$. When the fundamental mode dominates, as occurs for $\alpha \lesssim 0.08$, the fluctuations

are very strong. The amplitudes drop abruptly when the overtone mode becomes the dominant mode (at $M_A^{-1} \approx 0.1$). All our numerical evidence confirms that the flows have strong, nonlinear fluctuations when the physical parameters lie in the region below \mathcal{M}_A^{-1} in Figure 2. Above \mathcal{M}_A^{-1} the fluctuation amplitudes, while smaller than below, may still be appreciable. The parameter space covered by the simulations of Tóth & Draine does not cover the full range of plausible cooling-law slopes, and consequently several conclusions for our more realistic cooling function contradict their general results.

We end our discussion of single power-law cooling functions with comments about the robustness of the values of \mathcal{M}_A^{-1} with respect to changes in simulation parameters. As noted above, in the cases with $\alpha \leq -0.8$, for numerical convenience we use a value of the turnover temperature T_t ten times larger than the higher- α cases. We have verified in the case of $\alpha = -0.5$ that the selection of the dominant mode discussed below is insensitive to this increase in T_t . For smaller values of α , we are interested in the behavior at increasingly large magnetic fields. The effect on the dynamics of the cooling column should be negligible since T_t sets the thermal pressure of the cooled gas, but near the mode transition this thermal pressure is dominated by the magnetic pressure. For larger values $\alpha \gtrsim 0$, cases with small or zero magnetic fields are of interest, and the choice of final gas temperature does qualitatively affect the oscillations.

We believe that our choice of boundary conditions has little effect on the value of \mathcal{M}_A^{-1} . However, simulations of one-dimensional cooling shocks without magnetic fields by Strickland & Blondin (1995) suggest that boundary conditions may affect the stability or the dominant unstable mode. They offer as a possible explanation that a reflecting wall may return waves to the cooling region and interfere with the growth of unstable modes. We use the case of $\alpha = -0.5$ to check the dependence of \mathcal{M}_A^{-1} on boundary conditions. In order to remove the effect of reflected waves, we separate the cooling region from the wall with a column of quiescent gas large enough so that waves generated in the region of the shock are not reflected back to the cooling column during the simulation. We find no change in the qualitative behavior of cases on either side of our inferred \mathcal{M}_A^{-1} boundary.

Next we return to the more complex piecewise power-law cooling function shown in Figure 1. In Figure 4 we show the shock-velocity fluctuations for the cases mean shock speeds 150, 180, 210, and 240 km s^{-1} , each with Alfvén velocities 0, 2, 5, 10, and 20 km s^{-1} . The graphs show the shock velocity (in the frame of reference of the reflecting wall) as a function of time. Over this range of shock speeds, all $B = 0$ flows are unstable. Since the local slope of the cooling function varies, the lower shock speeds should be more unstable than the higher ones. We discuss the effects on stability, dominant mode, and oscillation amplitude as the magnetic field is increased.

Inspection of Figure 4 shows that (1) the fundamental mode dominates over most of the parameter space, (2) the amplitude of oscillations is nonlinear ($\sim 100\%$), and (3) the magnetic fields qualitatively alters the instability only at the lowest and highest shock speeds. In a few cases starting from near steady-state conditions, the growth rate of an unstable fundamental mode

is relatively slow, and the qualitative long-term behavior sets in only after 10–20 cyclic times. Before this occurs, the shock velocity oscillates with ever-increasing amplitude, and the variations in shock velocity are dominated by the overtone modes. We now discuss these observations in light of the conclusions drawn from the single power-law cooling simulations described above.

In two high-speed cases ($v_s = 240 \text{ km s}^{-1}$, $v_A = 10$ and 20 km s^{-1}), the magnetic field is sufficiently strong that the fundamental, but not the overtone, mode is stabilized. Under these circumstances the oscillations are noticeably smaller in amplitude than in the corresponding cases with lower magnetic fields. As expected for the first-overtone mode, the oscillation frequency is roughly three times that of the lower-magnetic-field 240 km s^{-1} cases, whose fundamental modes are unstable. (At high Alfvén Mach numbers the contribution of the magnetic field to the total pressure is small in gas that has not yet become cool and dense, and the cooling length and mode frequencies are not much altered from the $v_A = 0$ case.) The simulations show that $0.02 < \mathcal{M}_A^{-1} < 0.04$.

We may compare this with the results obtained using single power-law cooling. The relevant parameter for comparison is the power-law index α . At the shock temperature corresponding to 240 km s^{-1} , our cooling function locally has $\alpha \approx -0.1$. In that case, our power-law results (cf. Fig. 2) suggest that $\mathcal{M}_A^{-1} \approx 0.02$, roughly consistent with the 240 km s^{-1} simulations. The value of \mathcal{M}_A^{-1} is likely increased because the cooling function is steeper ($\alpha \approx -2.2$) in a wide range of temperatures below the shock temperature.

In one case ($v_s = 150 \text{ km s}^{-1}$, $v_A = 20 \text{ km s}^{-1}$) in Figure 4, the instability is absent; the oscillations shown are extremely small in amplitude and decaying. The simulations show that $0.07 < \{M_{A,F}^{-1}, M_{A,O}^{-1}\} < 0.13$. At a shock speed of 150 km s^{-1} , the shock temperature—if $B = 0$ —implies a local slope $\alpha \approx -2.2$. Although such a steep power law is not considered by the linear analysis of Tóth & Draine, extrapolation from their results indicates that $M_A^{-1} > 0.4$ would be required to stabilize the fundamental mode. In this case the observed stabilization is of a different nature: the upstream magnetic field is sufficiently large to reduce the shock temperature by more than 10% as compared with the $B = 0$ case. At this reduced temperature the cooling function is shallow ($\alpha = 0$) and less unstable. The combination of the curvature of the cooling function and the lowered shock temperature stabilizes fundamental and overtone modes in part of parameter space.

Finally, we come to the issue of stability over the large central range of shock speeds. We see no evidence of stabilization at $v_s = 180$ and 210 km s^{-1} for $v_A \leq 20 \text{ km s}^{-1}$ in Figure 4. We have performed additional simulations with larger magnetic fields ($v_A = 30$ and 40 km s^{-1}), and the results for the fundamental mode are summarized in Figure 5. The vertical line segments indicate constraints on the boundary of the fundamental-mode dominance. Arrows indicate that fundamental-mode stability requires *larger* magnetic fields than those we simulated. In the region below the lines marked in long dashes (drawn only for illustrative purposes) the fundamental mode dominates.

This picture is qualitatively different from that drawn by Tóth & Draine. For a very rough approximation to the interstellar-medium cooling function, they consider the simple broken power law shown in Figure 1. Their linear analysis then yields for the fundamental-mode stability limit the line drawn in short dashes in Figure 5. The results for our cooling function indicate that *much larger* magnetic fields are required to change the stability of the oscillations. The major difference between the cooling functions is that ours is much steeper (and hence more unstable) for shocks with $v_s \leq 200 \text{ km s}^{-1}$, but flatter (hence more stable) for higher-velocity shocks. Our picture agrees with the results from single power-law cooling above: the fundamental mode dominates the oscillations, and the oscillations have significant amplitudes in the presence of typical magnetic fields when $\alpha < 0$.

3. Conclusions

In our simulations the behavior of the overstability is determined by the typical shock temperature (hence the mean shock speed) and the upstream magnetic field. We divide the unstable cases into two categories: either the fundamental mode is unstable, or it is absent and the instability is dominated by the first overtone mode. The periods of these observed modes are roughly consistent with the prediction of linear perturbative analyses (Chevalier & Imamura 1982; Tóth & Draine 1993). Simulations with cooling functions (eq. [3]) that are truncated one-component power laws show a strong dependence on power-law index α and the Alfvén Mach number M_A^{-1} . The earlier simulations presented in Tóth & Draine (1993) all have $\alpha \geq 0$. For typical magnetic field strengths they found oscillations of limited ($\lesssim 10\%$) amplitudes dominated by overtone modes. For similar magnetic fields but $\alpha < 0$, we observe that the fundamental mode dominates and that the oscillations have large amplitudes. We note a significant drop in oscillation amplitude accompanying the switch from fundamental to overtone mode as the magnetic field is raised, as we show for the typical case of $\alpha = -0.8$. Even when the overtone mode dominates, the oscillations have substantial, nonlinear amplitudes. The linear analysis of Tóth & Draine yields the values of the reciprocal Mach numbers $M_{A,F}^{-1}$ and $M_{A,O}^{-1}$ at which the fundamental and overtone modes become linearly stable for the full range of α . Our nonlinear simulations do not disagree with the linear analysis: the reciprocal Mach number \mathcal{M}_A^{-1} at which the dominant oscillations change from fundamental to overtone mode differs significantly from $M_{A,F}^{-1}$, but always satisfies $\mathcal{M}_A^{-1} < M_{A,F}^{-1}$.

These single power-law cooling results explain our simulations that use a more realistic, piecewise power-law cooling function based on the results of Raymond et al. (1976). These simulations encompass mean shock speeds between 150 and 240 km s^{-1} and Alfvén velocities up to 20 km s^{-1} . Over most of the parameter space we observe large-amplitude fundamental-mode oscillations. The instability is so strong that quite substantial magnetic fields ($v_A \gtrsim 10 \text{ km s}^{-1}$) are required to change the qualitative behavior, and then only at the lowest and highest shock speeds. Again, we contrast our qualitative picture with the discussion of Tóth & Draine, who

consider a very rough model for the interstellar-medium cooling function with a single power law ($\alpha = -1/2$) above $T = 10^{5.3}$ K. With a linear analysis they find that magnetic fields of realistic amplitudes may stabilize radiative shocks with velocities up to approximately 175 km s^{-1} in the warm ionized medium and the warm neutral medium. For some cases, we find that fields *larger* than any we simulated—that is, $v_A > 40 \text{ km s}^{-1}$ —would be required to affect the stability behavior. The discrepancy between the two treatments points out that an accurate determination of the magnetic field required to stabilize shocks requires a more careful treatment of the cooling than the one we have attempted (see, for example, Innes 1992). However, the minimum magnetic field to stabilize the shock is quite dependent on the local power-law index α of the cooling function, and in any realistic treatment we expect α to vary over the velocity range of interest ($130 \text{ km s}^{-1} \lesssim \langle v_s \rangle \lesssim 250 \text{ km s}^{-1}$). We then anticipate that the stabilizing magnetic field will vary from case to case but could be quite large, as found in our simulations.

It must be noted that some aspects of gas behavior are not well modeled in our simulations. Perhaps the most prominent missing element is an accurate treatment of cooling, incorporating ionization and recombination in the cooling region, as well as in the upstream preshock gas and the cooled postshock gas. In particular, our cooling function only crudely mimics the turnoff of the cooling law upon recombination. There may as well be geometrical effects that require extending this work into two or three spatial dimensions. Further work will need to address one or more of these deficiencies.

We thank Edwin Salpeter and the anonymous referee for useful comments on drafts of this paper.

This research has been carried out at Cornell University with the generous support of the NSF (AST 91-19475) and NASA (NAGW-2224) under the LTSA program.

Some computations reported herein were carried out using the resources of the Cornell Theory Center, which receives major funding from the NSF and New York State, with additional support from ARPA, the National Center for Research Resources at the NIH, IBM Corporation, and other members of the Center’s Corporate Partnership Program.

REFERENCES

- Berger, M. J., & Colella, P. 1989, *J. Comput. Phys.*, 82, 64
- Chevalier, R. A., & Imamura, J. N. 1982, *ApJ*, 261, 543
- Gaetz, T. J., Edgar, R. J., & Chevalier, R. A. 1988, *ApJ*, 329, 927
- Imamura, J. N., Wolff, M. T., & Durisen, R. H. 1984, *ApJ*, 276, 667
- Innes, D. E. 1992, *A&A*, 256, 660
- Innes, D. E., Giddings, J. R., & Falle, S. A. E. G. 1987, *MNRAS*, 226, 67
- Kimoto, P. A., & Chernoff, D. F. 1997, *ApJ*, 485, 274
- Langer, S. H., Chanmugam, G., & Shaviv, G. 1981, *ApJ*, 245, L23
- Raymond, J. C., Cox, D. P., & Smith, B. W. 1976, *ApJ*, 204, 290
- Strickland, R., & Blondin, J. M. 1995, *ApJ*, 449, 727
- Tóth, G., & Draine, B. T. 1993, *ApJ*, 413, 176
- Walder, R., & Folini, D. 1996, *A&A*, 315, 265
- Zalesak, S. T. 1979, *J. Comput. Phys.*, 31, 335

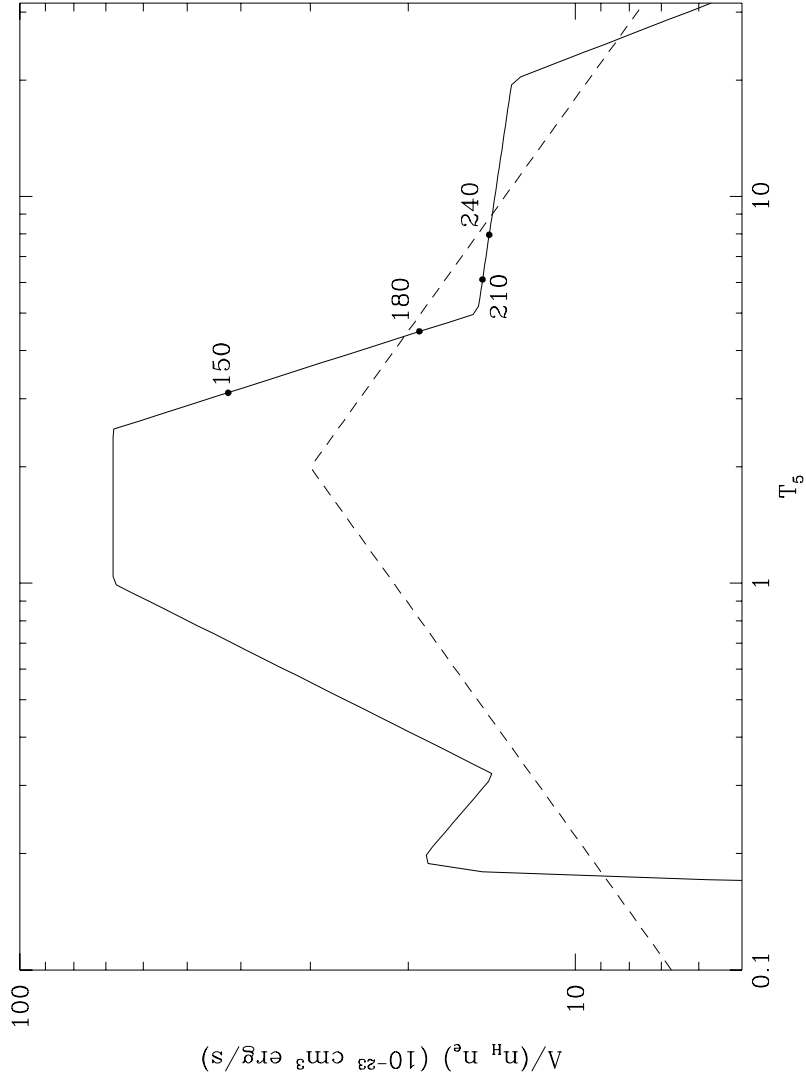


Fig. 1.— The simulations use the cooling function indicated by the solid line, a piecewise power-law fit to the result of Raymond et al. (1976), and arranged to turn off at low temperatures. The dashed line shows the simple function adopted by Tóth & Draine (1993) for application to the interstellar medium. The four dots indicate the postshock gas temperatures for shocks moving at 150, 180, 210, and 240 km s⁻¹.

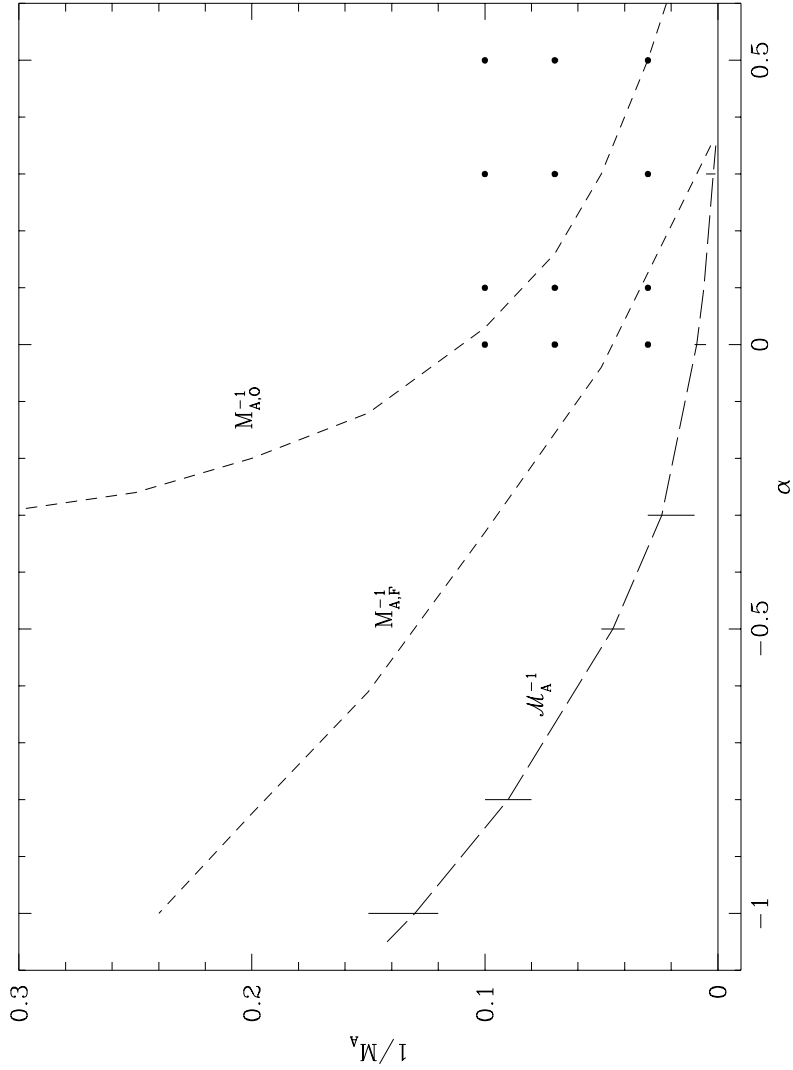


Fig. 2.— From our simulations with power-law cooling, we find that the fundamental mode dominates the instability roughly in the region below the long dashed lines in (α, M_A^{-1}) parameter space, where α is the power-law index. (The short line segments indicate simulations between which the fundamental mode becomes stable.) The short dotted lines indicate curves of marginal stability for the fundamental ($M_{A,F}^{-1}$, lower) and overtone ($M_{A,O}^{-1}$, upper) modes as calculated by Tóth & Draine (1993). The dots indicate the twelve simulations discussed by Tóth & Draine.

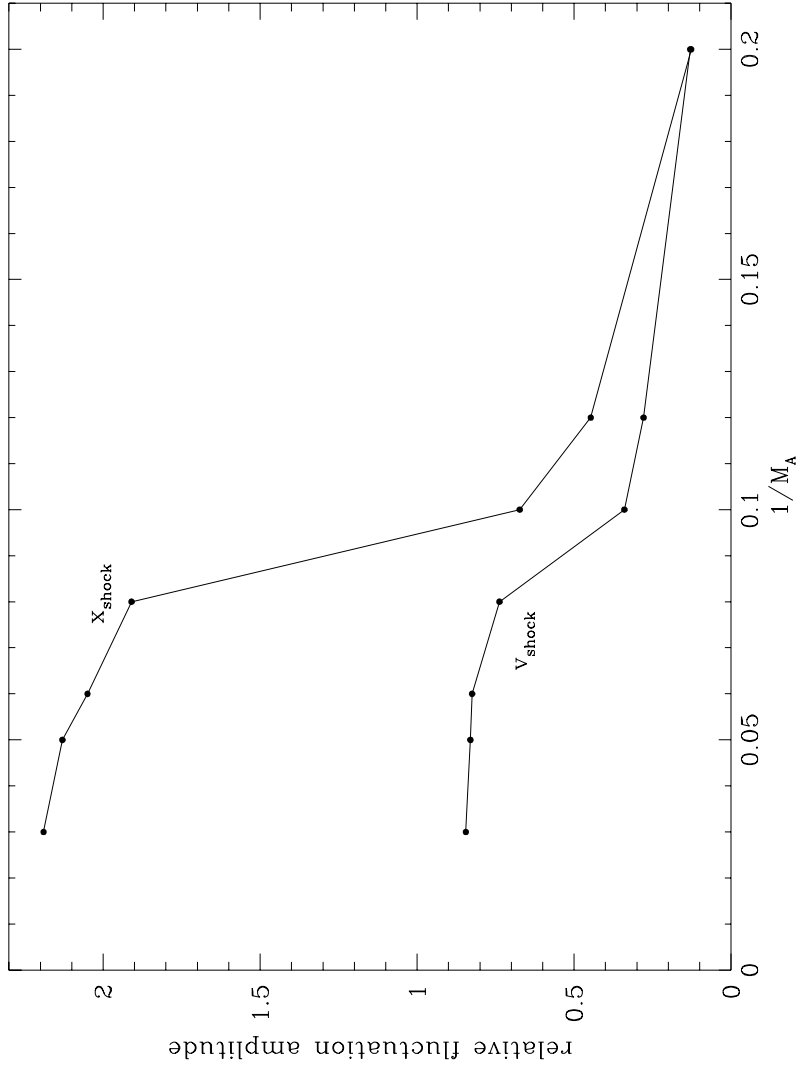


Fig. 3.— Typical sizes of shock fluctuations (relative to steady-state values) as a function of reciprocal Alfvén Mach number, for power-law cooling (eq. [3]) with $\alpha = -0.8$. The fundamental mode dominates for $M_A^{-1} \leq 0.08$; and the overtone, for $M_A^{-1} \geq 0.1$.

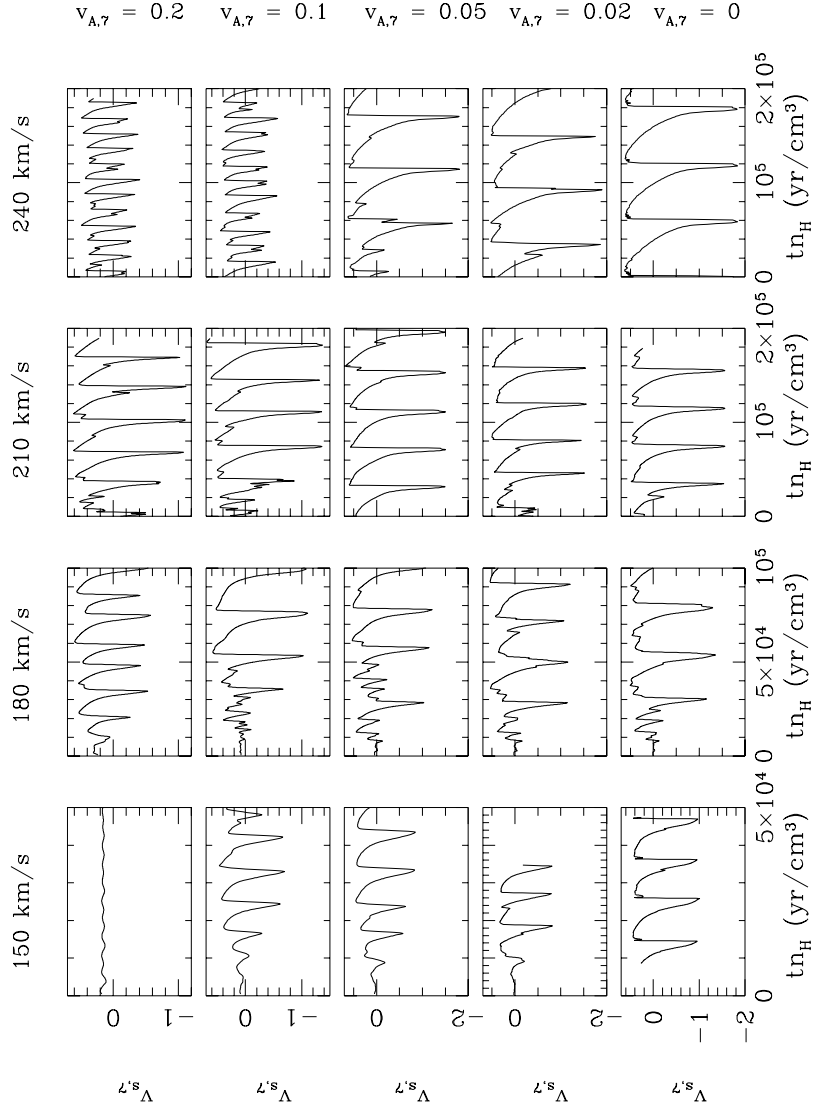


Fig. 4.— Shock velocity (in units of 100 km s^{-1}) as a function of time for mean shock speeds 150, 180, 210, and 240 km s^{-1} (from left to right) and upstream Alfvén velocities 0, 2, 5, 10, and 20 km s^{-1} (from bottom to top).

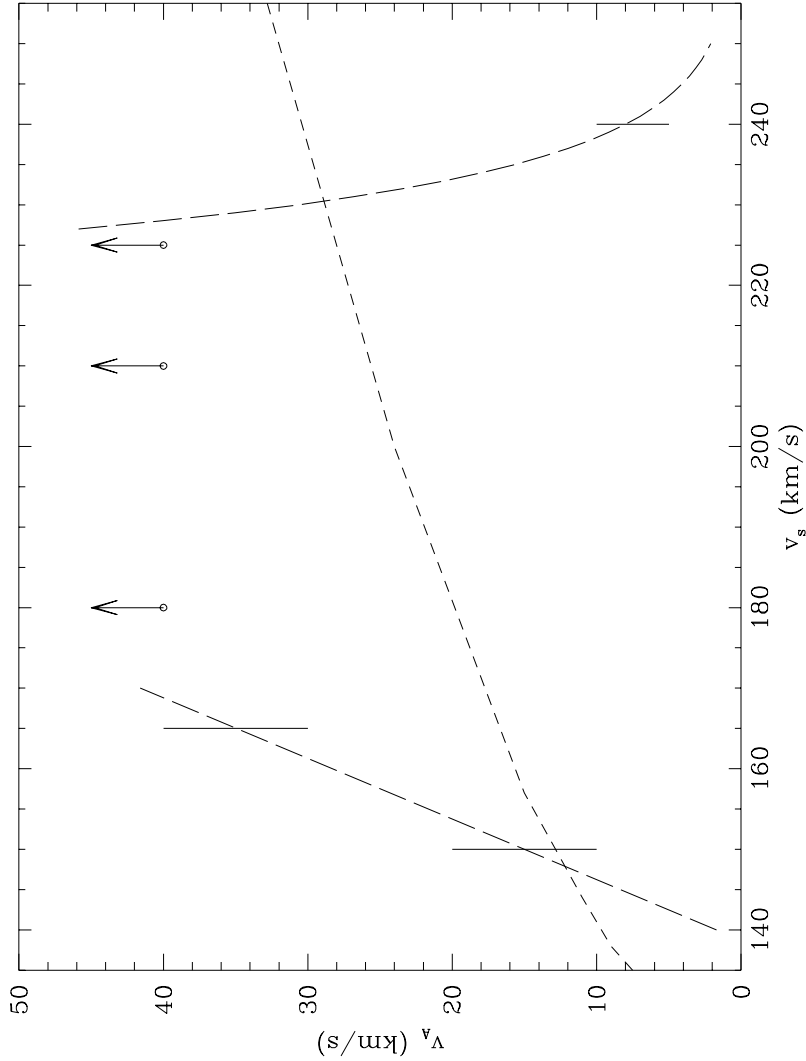


Fig. 5.— From our simulations we find the fundamental mode is unstable roughly in the region below the long dashed lines. (The short line segments indicate simulations between which the fundamental mode becomes stable; the transition happens at magnetic fields above the points marked with arrows.) For comparison, the region below the short dashed lines is found to be unstable to the fundamental mode by Tóth & Draine (1993). The difference is attributable to the different cooling function (cf. fig. 1).

Table 1: Average shock speeds in simulations

Intended average (km s^{-1})	Upstream Alfvén velocity (km s^{-1})	Inflow velocity (km s^{-1})	Actual average (relative) (km s^{-1})
150	0	149	150 ± 1
150	2	148	149 ± 1
150	5	146	151 ± 3
150	10	142	150 ± 1
150	20	134	150
180	0	179	181 ± 1
180	2	178	182 ± 2
180	5	176	181 ± 1
180	10	172	180 ± 2
180	20	157	177 ± 2
210	0	209	210 ± 1
210	2	208	210 ± 1
210	5	206	210 ± 1
210	10	202	211 ± 3
210	20	195	210 ± 2
240	0	239	240 ± 1
240	2	238	238 ± 2
240	5	236	238 ± 3
240	10	232	240 ± 1
240	20	225	240 ± 2

Table 2: Typical parameters of shock-velocity oscillations without magnetic fields

Mean shock velocity (km s^{-1})	Velocity fluctuation (km s^{-1})	Fluctuation period ^a (yr)	Linear period τ_F (yr)
130	80	4 400	4 000
140	95	7 000	4 500
150	140	11 000	5 600
160	140	13 000	7 900
170	160	17 000	11 000
180	160	20 000	16 000
190	160	30 000	22 000
200	160	34 000	29 000
210	200	40 000	35 000
225	210	47 000	43 000
240	240	63 000	53 000

^a $n_H = 1 \text{ cm}^{-3}$; all times vary as n_H^{-1}